Synthesis and Characterization of Some Derivatives of Lupinine and Aminolupinine. Collision Induced Dissociation Mass Spectrometry Studies of Protonated Molecules.

Rust T. Tlegenov,[1] Jaana M. H. Pakarinen,[2] Larisa Oresmaa,[2] Markku Ahlgrén,[2] and Pirjo Vainiotalo[2]*

[1]Karakalpak State University, Universitetskaya 1, 742012 Nukus City, Republic of Karakalpakstan

[2]University of Joensuu, Department of Chemistry, P. O. Box 111, FI-80101 Joensuu, Finland
Fax: +358 (13) 2513360.
E-mail: pirjo.vainiotalo@joensuu.fi
Received November 30, 2006

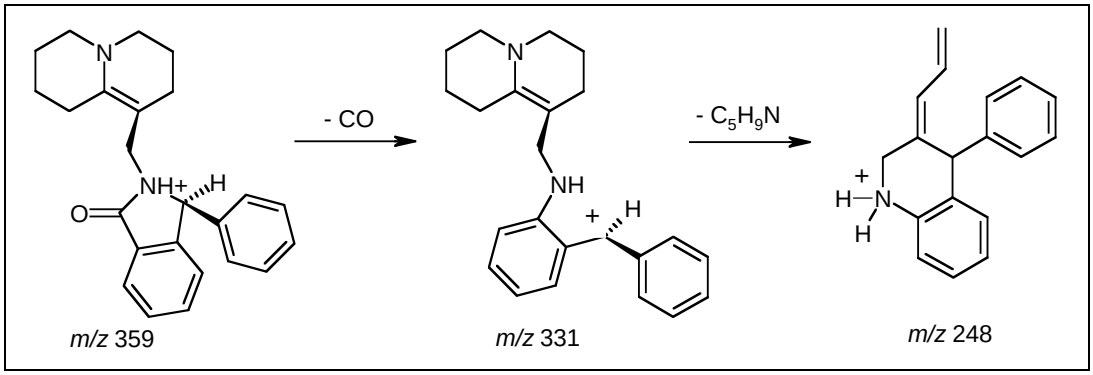

Some ester, amide and thioether derivatives of lupinine, aminolupinine and bromolupinine were synthesized and characterized in order to search biologically active compounds. The protonated molecules were studied by tandem mass spectrometry using collision induced dissociation (CID) technique in order to find out how different structural features and functional groups in different quinolizidine derivatives influence fragmentation behavior. Some theoretical calculations were also made to clarify the conformations of neutral and protonated molecules, to reveal the fragmentation routes and the product ions obtained. The functional groups clearly directed the fragmentations although the typical fragments for lupinine were still observed in all the cases. Theoretical calculations were in agreement with observed fragmentations and greatly helped interpretation of the CID spectra.

J. Heterocyclic Chem., **44**, 1339 (2007).

INTRODUCTION

A number of alkaloids having bicyclic quinolizidine ring structure have been isolated from a variety of natural sources and have proven to possess considerable biological activity [1]. One of the simplest molecules known to contain this skeleton is lupinine ([1-*R-trans*]-octahydro-2*H*-quinolizine-1-methanol (**1**)), which is one of the major alkaloids of *Anabasis aphylla* and some species of *Lupinus*. Lupinine has various biological activities [2] *e.g.* it possesses an anticholinesterase activity [3] and is used in medicine for preparing substances with local anesthetic action [4]. Lupinine is a crystal organic base which crystallizes from petroleum ether as rhombic crystals. The presence of hydroxy group in the molecule enables the further conversion into various derivatives and there are several studies concerning the synthesis of lupinine and its derivatives. [5-8].

In the present work, some ester, amide and thioether derivatives of lupinine, aminolupinine (**2**) and bromolupinine (**5**) were synthesized and characterized in order to search biologically active compounds. The compounds were synthesized according to Scheme 1.

RESULTS AND DISCUSSION

Because the compounds synthesized form a nice series of quinolizidine derivatives the protonated molecules were studied also by tandem mass spectrometry using collision induced dissociation (CID) technique. This procedure gives us a possibility to find out how different structural features and functional groups in different quinolizidine derivatives influence on fragmentation behavior. Some theoretical calculations were also made to clarify the conformations of neutral and protonated molecules, to reveal the fragmentation routes and the product ions obtained.

The biological activity of the compounds synthesized was tested by TAACF (Tuberculosis Antimicrobial Acquisition and Coordinating Facility) against *Mycobacterium tuberculosis* using Bactec assay [9]. The results are presented in Table 2.

Scheme 1

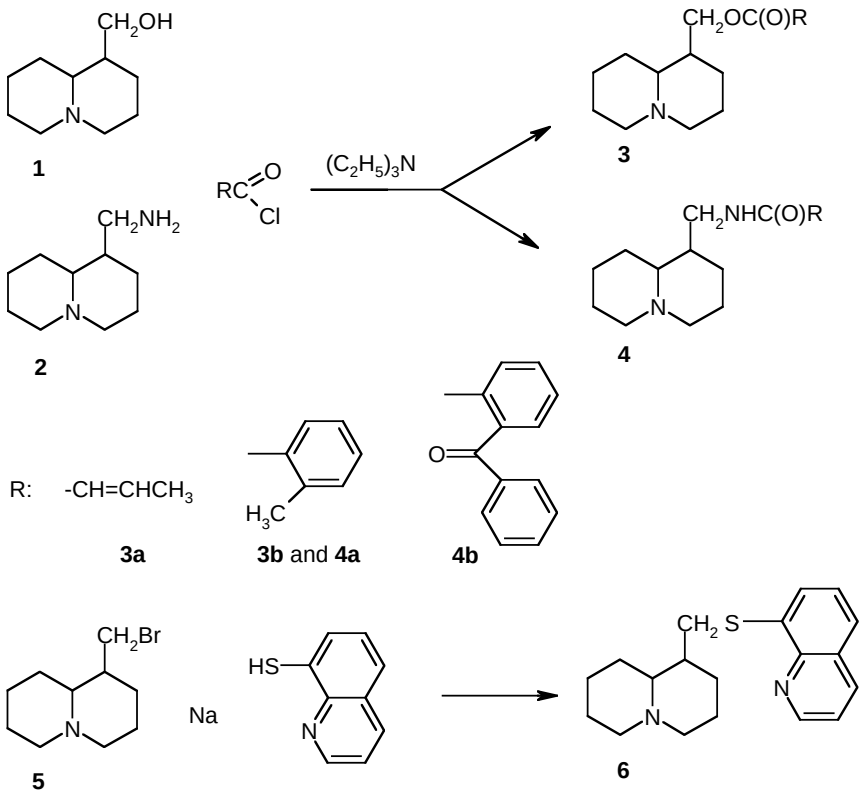

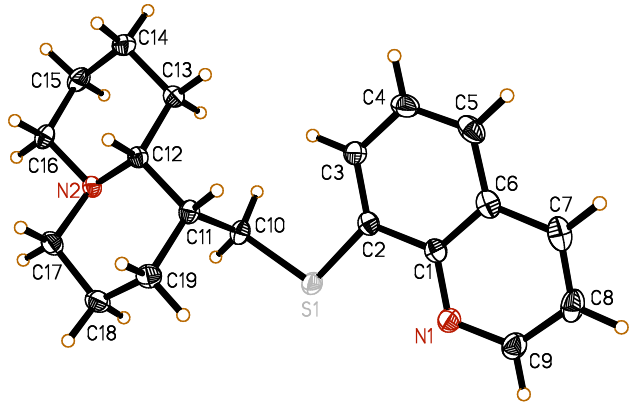

Figure 1. Molecular structure and atomic numbering scheme for compound **6**.

Table 1

Bond lengths [Å] and angles [deg] for compound **6**.

S(1)-C(2)	1.763(1)	C(2)-S(1)-C(10)	103.2(1)
S(1)-C(10)	1.816(1)	C(9)-N(1)-C(1)	117.6(1)
N(1)-C(9)	1.321(2)	C(17)-N(2)-C(16)	107.3(1)
N(1)-C(1)	1.370(2)	C(17)-N(2)-C(12)	110.9(1)
N(2)-C(17)	1.469(2)	C(16)-N(2)-C(12)	110.0(1)
N(2)-C(16)	1.471(2)	N(1)-C(1)-C(6)	122.3(1)
N(2)-C(12)	1.475(2)	N(1)-C(1)-C(2)	118.0(1)
C(1)-C(6)	1.420(2)	C(6)-C(1)-C(2)	119.7(1)
C(1)-C(2)	1.429(2)	C(3)-C(2)-C(1)	118.6(1)
C(2)-C(3)	1.378(2)	C(3)-C(2)-S(1)	125.5(1)
C(3)-C(4)	1.413(2)	C(1)-C(2)-S(1)	15.9(1)
C(3)-H(3)	0.9500	C(2)-C(3)-C(4)	121.1(1)
C(4)-C(5)	1.365(2)	C(2)-C(3)-H(3)	119.4
C(4)-H(4)	0.9500	C(4)-C(3)-H(3)	119.4
C(5)-C(6)	1.415(2)	C(5)-C(4)-C(3)	121.2(1)
C(5)-H(5)	0.9500	C(5)-C(4)-H(4)	119.4
C(6)-C(7)	1.419(2)	C(3)-C(4)-H(4)	119.4
C(7)-C(8)	1.362(2)	C(4)-C(5)-C(6)	119.5(1)
C(7)-H(7)	0.9500	C4-C(5)-H(5)	120.2
C(8)-C(9)	1.412(2)	C(6)-C(5)-H(5)	120.2
C(8)-H(8)	0.9500	C(5)-C(6)-C(7)	122.6(1)
C(9)-H(9)	0.9500	C(5)-C(6)-C(1)	119.8(1)
C(10)-C(11)	1.538(2)	C(7)-C(6)-C(1)	117.6(1)
C(10)-H(10A)	0.9900	C(8)-C(7)-C(6)	119.6(1)
C(10)-H(10B)	0.9900	C(8)-C(7)-H(7)	120.2
C(11)-C(19)	1.532(2)	C(6)-C(7)-H(7)	120.2
C(11)-C(12)	1.545(2)	C(7)-C(8)-C(9)	118.7(1)
C(11)-H(11)	1.0000	C(7)-C(8)-H(8)	120.6
C(12)-C(13)	1.535(2)	C(9)-C(8)-H(8)	120.6
C(12)-H(12)	1.0000	N(1)-C(9)-C(8)	124.2(1)
C(13)-C(14)	1.531(2)	N(1)-C(9)-H(9)	117.9
C(13)-H(13A)	0.9900	C(8)-C(9)-H(9)	117.9
C(13)-H(13B)	0.9900	C(11)-C(10)-S(1)	115.0(1)
C(14)-C(15)	1.520(2)	C(11)-C(10)-H(10A)	108.5
C(14)-H(14A)	0.9900	S(1)-C(10)-H(10A)	108.5
C(14)-H(14B)	0.9900	C(11)-C(10)-H(10B)	108.5
C(15)-C(16)	1.519(2)	S(1)-C(10)-H(10B)	108.5
C(15)-H(15A)	0.9900	H(10A)-C(10)-H(10B)	107.5
C(15)-H(15B)	0.9900	C(19)-C(11)-C(10)	111.9(1)
C(16)-H(16A)	0.9900	C(19)-C(11)-C(12)	110.0(1)
C(16)-H(16B)	0.9900	C(10)-C(11)-C(12)	112.9(1)
C(17)-C(18)	1.517(2)	C(19)-C(11)-H(11)	107.3
C(17)-H(17A)	0.9900	C(10)-C(11)-H(11)	107.3

Table 1 (continued)

Table 1 (continued)

C(17)-H(17B)	0.9900	C(12)-C(11)-H(11)	107.3
C(18)-C(19)	1.528(2)	N(2)-C(12)-C(13)	110.0(1)
C(18)-H(18A)	0.9900	N(2)-C(12)-C(11)	111.5(1)
C(18)-H(18B)	0.9900	C(13)-C(12)-C(11)	112.8(1)
C(19)-H(19A)	0.9900	N(2)-C(12)-H(12)	107.4
C(19)-H(19B)	0.9900	C(13)-C(12)-H(12)	107.4
C(11)-C(12)-H(12)	107.4	C(14)-C(13)-C(12)	111.8(1)
C(14)-C(13)-H(13A)	109.3	C(12)-C(13)-H(13A)	109.3
C(14)-C(13)-H(13B)	109.3	C(12)-C(13)-H(13B)	109.3
H(13A)-C(13)-H(13B)	107.9	C(15)-C(14)-C(13)	108.5(1)
C(15)-C(14)-H(14A)	110.0	C(13)-C(14)-H(14A)	110.0
C(15)-C(14)-H(14B)	110.0	C(13)-C(14)-H(14B)	110.0
H(14A)-C(14)-H(14B)	108.4	C(16)-C(15)-C(14)	109.3(1)
C(16)-C(15)-H(15A)	109.8	C(14)-C(15)-H(15A)	109.8
C(16)-C(15)-H(15B)	109.8	C(14)-C(15)-H(15B)	109.8
H(15A)-C(15)-H(15B)	108.3	N(2)-C(16)-C(15)	112.8(1)
N(2)-C(16)-H(16A)	109.0	C(15)-C(16)-H(16A)	109.0
N(2)-C(16)-H(16B)	109.0	C(15)-C(16)-H(16B)	109.0
H(16A)-C(16)-H(16B)	107.8	N(2)-C(17)-C(18)	112.1(1)
N(2)-C(17)-H(17A)	109.2	C(18)-C(17)-H(17A)	109.2
N(2)-C(17)-H(17B)	109.2	C(18)-C(17)-H(17B)	109.2
H(17A)-C(17)-H(17B)	107.9	C(17)-C(18)-C(19)	109.9(1)
C(17)-C(18)-H(18A)	109.7	C(19)-C(18)-H(18A)	109.7
C(17)-C(18)-H(18B)	109.7	C(19)-C(18)-H(18B)	109.7
H(18A)-C(18)-H(18B)	108.2	C(18)-C(19)-C(11)	111.3(1)
C(18)-C(19)-H(19A)	109.4	C(11)-C(19)-H(19A)	109.4
C(18)-C(19)-H(19B)	109.4	C(11)-C(19)-H(19B)	109.4
H(19A)-C(19)-H(19B)	108.0		

10^{-4}) having oxonium ion structure as a consequence of the elimination of neutral lupinine or aminolupinine. As expected these ions further loose CO (28 Da) giving rise to the *m/z* 91 ions ($C_7H_7^+$, calcd. 91.05423, found 91.05382, diff. 4.1×10^{-4}). Most of the $[M+H]^+$ ions seem to fragment *via* this pathway.

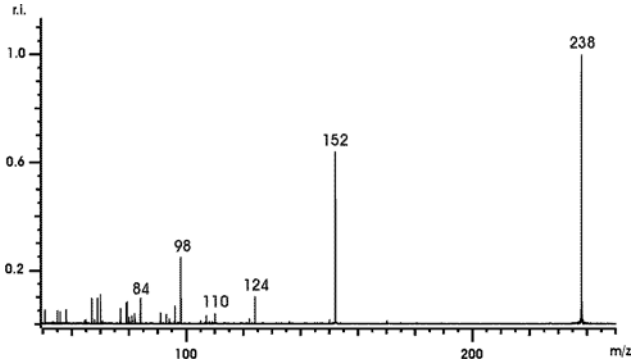

Figure 2. Collision induced dissociation spectrum of the $[M+H]^+$ ion (*m/z* 238) generated from compound **3a**.

Table 2

The biological activity of the compounds against *Mycobacterium tuberculosis* using Bactec assay.

Compound	Assay	MIC (μg/mL)	% Inhibition	Comment
3a	Bactec	>12.5	55	MIC RMP=0.25 μg/mL vs.*M.tuberculosis*
3b	Bactec	>12.5	57	MIC RMP=0.25 μg/mL vs.*M.tuberculosis*
4a	Bactec	>12.5	45	MIC RMP=0.25 μg/mL vs.*M.tuberculosis*
4b	Bactec	>12.5	34	MIC RMP=0.25 μg/mL vs.*M.tuberculosis*
6	Bactec	>12.5	58	MIC RMP=0.25 μg/mL vs.*M.tuberculosis*

Depending on the group attached to the heteroatom situated on the side chain of the octahydroquinolizine skeleton the protonated molecules, $[M+H]^+$ ions, can be divided into three categories in their fragmentation behavior. Protonated lupinine initially lost water giving rise to the $[C_{10}H_{18}N]^+$ ions at *m/z* 152 (calcd. 152.14338, found 152.14221, diff. 1.2×10^{-3}). These ions further eliminated C_2H_4, C_3H_6, C_4H_6 and C_5H_8 fragments forming the ions at *m/z* 124 ($C_8H_{14}N^+$, calcd. 124.11208, found 124.11128, diff. 8.0×10^{-4}), 110 ($C_7H_{12}N^+$, calcd. 110.09643, found 110.09562, diff. 8.0×10^{-4}), 98 ($C_6H_{12}N^+$, calcd. 98.09643, found 98.09594, diff. 4.9×10^{-4}) and 84 ($C_5H_{10}N^+$, calcd. 84.08078, found 84.08025, diff. 5.3×10^{-4}), respectively. The $[M+H]^+$ ions generated from compounds **3a** and **6** behaved analogously eliminating neutral carboxylic acid or thiol giving rise to the same fragment ions as lupinine (Figure 2). In addition to the ions mentioned above, *o*-methyl benzoic acid derivative compounds **3b** and **4a** also formed the *m/z* 119 ions ($C_8H_7O^+$, calcd. 119.04914, found 119.04874, diff. $4.0 \times$

Protonated compound **4b** showed most interesting fragmentation behavior which differed considerably from that of other compounds studied because besides the fragmentations mentioned above abundant elimination of water was observed. CID measurements made as a function of collision energy revealed that this was the lowest energy fragmentation giving rise to abundant fragment ions already at low collision energies. When the collision energy was increased two other fragmentation pathways mentioned above became apparent meaning the formation of the ions at *m/z* 209 (oxonium ion) and 152. The water elimination product at *m/z* 359 decomposed further forming the ions at *m/z* 331, 248 and 150 (Figure 3, Scheme 2). This behavior can be explained by assuming the structure presented in Scheme 2 for the *m/z* 359 ion. The formation of the *m/z* 150 ion is the most favorable requiring the elimination of neutral 5-phenyl 2-benzopyrrolidinone. The *m/z* 331 ($C_{23}H_{27}N_2^+$, calcd. 331.21688, found 331.21856, diff. 1.7×10^{-3}) is formed through the elimination of CO from *m/z* 359 leading to the

benzyl ion structure where the positive charge can be delocalized into two phenyl rings. The ion is decomposing further to the ions at *m/z* 248 ($C_{18}H_{18}N^+$, calcd. 248.14338, found 248.13912, diff. 4.3×10^{-3}) by losing neutral C_5H_9N as determined using accurate mass measurement and MS^3 experiments (Scheme 2). The fragment ion structures presented in Scheme 2 are verified also using theoretical calculations.

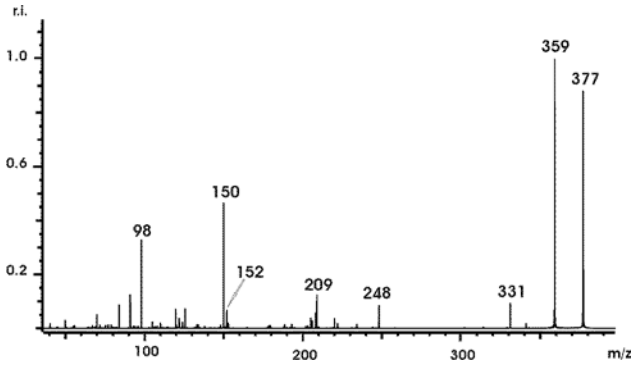

Figure 3. Collision induced dissociation spectrum of the $[M+H]^+$ ion (*m/z* 377) generated from compound **4b**.

Scheme 2

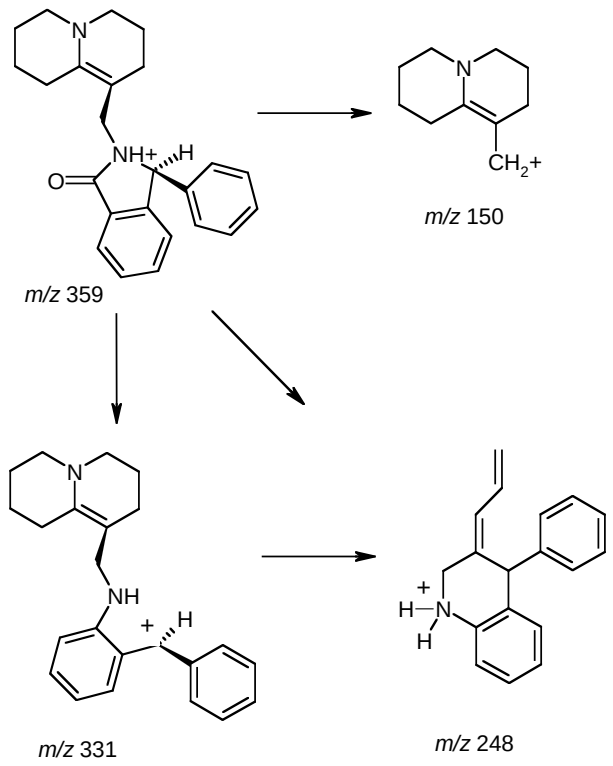

The different fragmentation pathways obtained for the compounds by CID gave an impact to study the compounds also using theoretical *ab initio* and hybrid density functional calculations. From all the experimentally studied compounds, three different compounds, namely **3a**, **4a** and **4b**, were chosen. These were the compounds which all were noticed to fragment in their own characteristic way. Different neutral and protonated conformations with the stable chair conformation of bicyclic quinolizidine ring structure and equatorial position of the side chain substituent were chosen and optimized to the minima at the HF/3-21G level of theory. The final calculations for the most stable neutral conformations and the most interesting protonated forms were performed at the B3LYP/6-31G(d) level of theory (Figure 4). Generally, the protonation of the quinolizidine ring nitrogen produced the most stable conformations for protonated compounds **3a**, **4a** and **4b**. Also, other possible heteroatom protonation sites were examined to evaluate the changes to the conformations and to explain experimentally discovered different fragmentation products. The bond distances in text refer to the calculations done at the B3LYP/6-31G(d) level of theory.

The compound **3a** was observed to fragment under CID correspondingly to lupinine. The theoretical results were found to confirm the experimental results. The protonation of the carbonyl oxygen of the substituent increased the $-CH_2-$ O- bond from 1.445 Å to 1.505 Å also suggesting the breakage of the bond and production the ion of *m/z* 152.

The second calculationally interesting compound was **4a** because of its additional fragmentation pathway compared to lupinine. The change of the ester substituent to amide substituent can not be the only explanation to the appearance of oxonium ion ($C_8H_5O^+$) at *m/z* 119 because also the compound **3b** having an ester substituent was found to fragment similarly. The explanation must be the formed stable aryl oxonium ion where the charge may delocalize to the phenyl ring. The protonation of amide nitrogen causes the bond lengths of $-CH_2-$ NH- and –NH – CO- to increase from 1.459 Å and 1.371 Å to 1.517 Å and 1.596 Å and explains the easy fragmentation of the bonds to produce both the ions of *m/z* 152 and *m/z* 119. On the other hand, the protonation of amide oxygen seems to favor the formation of the ion *m/z* 152.

Interestingly, for compound **4b** which showed notable different fragmentation behavior compared to other compounds studied the most stable neutral conformation was found to be the structure where the intramolecular hydrogen bond (1.906 Å) exists between the amide nitrogen and carbonyl oxygen (Ph-CO-Ph) of the side chain substituent (Figure 4). The protonation of the amide nitrogen stabilizes even more the hydrogen bond (1.594 Å) and increases the $(Ph)_2C=O$ bond (from 1.231 Å to 1.245 Å) suggesting the fragmentation of water under collision induced dissociation. Also the fragmentation product of *m/z* 359 was calculated to have the stable conformation and a long $-CH_2-$ NH- bond (1.612 Å)

producing readily the fragment ion *m/z* 150 (see Scheme 2). Also two other fragment ions from *m/z* 359, namely *m/z* 331 and *m/z* 248 were verified calculationally.

EXPERIMENTAL

Mass Spectrometry. Electrospray ionization (ESI) mass spectra were measured using a Fourier transform ion cyclotron resonance mass spectrometer (Bruker BioApex 47e, Bruker Daltonics, Billerica, USA), equipped with a 4.7 Tesla, 160 mm bore superconducting magnet (Magnex Scientific Ltd., Abingdon, UK), Infinity™ cell and interfaced to an electrospray ionization source (Bruker Apollo ESI source). The instrument was calibrated externally using a water:acetonitrile solution of sodium trifluoroacetate, as introduced by Moini *et. al*. [10]. The sample solution was continuously introduced into the interface sprayer by a syringe infusion pump at a flow rate of 50 μl/h under atmospheric pressure. The compounds were first dissolved into ethanol at a concentration of 1 mg/mL. These solutions were diluted with 100:1 methanol:acetic acid solution to the final concentration of 5 μM. In collision-induced dissociation (CID) experiments, collisionally cooled precursor ions were isolated in the ICR cell by the CHEF isolation technique [11]. The ions were excited and allowed to undergo collisions with pulsed argon gas, and after dissociation delay time the spectrum was collected.

Crystallographic data. Compound **6** were collected by on a Nonius Kappa CCD diffractometer using graphite-monochromated Mo-Kαradiation (λ = 0.71073 Å). The intensity data were corrected for Lorenz and polarization effects, and an empirical absorption correction was applied to the net intensities. The structure was solved by direct methods using SHELXS-97 [12] and refined using SHELXL-97 [13].

Crystallographic summary: $C_{19}H_{26}N_2S$, M_r = 312.46, Monoclinic, $P2_1$, a = 8.5101(2), b = 10.5297(2), c = 9.8836(2), β = 114.034(1), V = 808.87(3), Z = 2, D_c = 1.283 g/cm^3, μ = 0.199 mm^{-1}, Flack χ parameter = -0.04(4), F(000) = 336, T = 120 K, conventional R(F) = 0.0265 for 3503 unique reflections I > 2σ(I) and wR(F^2) = 0.0675 for all 3648 unique data.

Computational method. *Ab initio* and hybrid density functional (DFT) calculations were performed with the Gaussian03 [14] series of programs on Sun Fire 25K hardware on the Center for Scientific Computing (CSC) in Espoo and on Intel Pentium 4 Xeon hardware at the University of Joensuu. First, different conformations for both the neutral and different protonated molecules (**3a**, **4a** and **4b**) were calculated employing a Hartree-Fock (HF) procedure using the 3-21G basis set. Final optimized geometries were obtained using the density functional calculations (DFT) at the B3LYP/6-31G(d) level of theory. Harmonic frequency analysis was done also using the B3LYP/6-31G(d) basis set and the structures correspond to the true equilibrium configuration as no imaginary frequencies were obtained. The visualization of structures was performed with GaussView 3.0.[15]

^{1}H NMR spectra were recorded on a Bruker Avance 250 NMR spectrometer.

The starting lupinine was isolated from commercial grade anabasine sulphate [1]

General procedure for preparation of the esters (3a and 3b). A mixture of lupinine 3.4 g (0.02 mol), triethylamine 2,5 g and absolute benzene 80 ml was cooled to 0 °C. Acid chloride 0.021 mol in absolute benzene 20 ml was added dropwise during 30 min. The reaction mixture was stirred at 70-75 °C for 4-5 h. After cooling the triethylamine hydrochloride precipitated and was filtered off and washed with benzene. The filtrate was evaporated in vacuum. The raw product was purified by column chromatography (Al_2O_3, eluent benzene-chloroform-ethanol 18:15:1).

But-2-enoic acid octahydro-quinolizin-1-ylmethyl ester (3a). The compound was prepared according to the general method, yield 3.32 g (79 %); R_f= 0.66 (chloroform-ethanol 2:1); ^{1}H NMR (D_2O): δ= 1.38-2.32 (14H); 2.86 (2H); 3.98-4.36 (2H); 5.88 (1H), 7.03 (1H); MS (ESI): calcd. for $C_{14}H_{24}N_1O_2$ $[M+H]^+$ = 238.18016. Found $[M+H]^+$ = 238,18008. Diff. 8.0 × 10^{-5}. *Anal.* Calcd. for $C_{14}H_{23}N_1O_2$: C, 70.76; H, 9.68; N, 5.89. Found C, 70.42 H, 9.33; N, 6.0.

2-Methyl-benzoic acid octahydro-quinolizin-1-ylmethyl ester (3b). The compound was prepared according to the general method, yield 4.88 g (85 %); R_f= 0.80 (chloroform-ethanol 2:1); mp. 32-34 °C; ^{1}H NMR (MeOD): δ= 1.50-2.07 (14H); 2.58 (3H); 3.04 (2H); 4.24-4.63 (2H); 7.27-7.32 (2H); 7.44 (1H); 7.88-7.90 (1H); MS (ESI): calcd. for $C_{18}H_{26}N_1O_2$ $[M+H]^+$ = 288.19581. Found $[M+H]^+$ = 288.19548. Diff. 3.3 × 10^{-4}. *Anal.* Calcd. for $C_{18}H_{25}N_1O_2$: C, 75.15; H, 8.69; N, 4.86. Found C, 75.34; H, 8.94; N, 4.86.

General procedure for preparation of the amides (4a and 4b). A mixture of aminolupinine 3.36 g (0.02 mol), triethylamine 2,5 g and absolute ether 80 ml was cooled to 0 °C. Acid chloride 3.1 g (0.021 mol) in absolute benzene 20 ml was added dropwise during 1 h. The reaction mixture was refluxed for 3 h. After cooling the triethylamine hydrochloride precipitated and was filtered off and washed with ether. The filtrate was evaporated in vacuum. The raw product was purified by column chromatography (SiO_2, eluent chloroform:ethanol 2:1).

2-Methyl-*N*-(octahydro-quinolizin-1-ylmethyl)-benzamide (4a). The compound was prepared according to the general method, yield 4.58 g (80 %); R_f= 0.62 (chloroform-ethanol 2:1); mp. 119-120 °C; ^{1}H NMR ($CDCl_3$): δ= 1.25-2.09 (14H); 2.48 (3H); 2.80 (2H); 3.56-3.72 (2H); 7.16-7.38 (4H); MS (ESI): calcd. for $C_{18}H_{27}N_2O$ $[M+H]^+$ = 287.21179. Found $[M+H]^+$ = 287.21188. Diff. 9.0 × 10^{-5}. *Anal*. Calcd. for $C_{18}H_{26}N_2O$: C, 75.41; H, 9.08; N, 9.77. Found C, 75.13; H, 9.22; N, 10.11.

2-Benzoyl-*N*-(octahydro-quinolizin-1-ylmethyl)-benzamide (4b). The compound was prepared according to the general method, yield 3.6 g (68.6 %); R_f= 0.62 (chloroform-ethanol 2:1); ^{1}H NMR ($CDCl_3$): δ= 1.25-1.96 (14H); 2.85 (2H); 3.60-3.79 (2H); 7.30-7.62 (9H); MS (ESI): calcd. for $C_{24}H_{30}N_2O_2$ $[M+H]^+$ = 377.22236. Found $[M+H]^+$ = 377.22219. Diff. 1.7 × 10^{-4}. *Anal.* Calcd. for $C_{24}H_{29}N_3O_2$: C, 73.6; H, 7.4; N, 10.4. Found C, 73.4; H, 7.0; N, 10.0.

8-(Octahydro-quinolizin-4-ylmethylsulfanyl)-quinoline (6). The suspension of 8-mercaptoquinoline, sodium and benzene was heated to reflux and bromolupinine (**5**) was added. The reaction mixture was heated for 6 h. After the reaction sodium bromide precipitated and was filtered off. Benzene 100 ml was added to the filtrate and washed few times with 10 % NaOH solution. The organic phase was dried over Na_2SO_4. The solvent was evaporated on vacuum resulting oil which turned into colorless crystals during the storage. The product was recrystallized from acetone. Yield 2.81 g (45 %); R_f= 0.39 (chloroform-ethanol 2:1); mp. 111-112 °C; ^{1}H NMR ($CDCl_3$): δ= 1.48-2.02 (14H); 2.89 (2H); 3.20-3.34 (2H); 7.41-7.55 (4H); 8.10-8.13 (1H); 8.93-8.95 (1H); MS (ESI): calcd. for $C_{19}H_{25}N_2S$

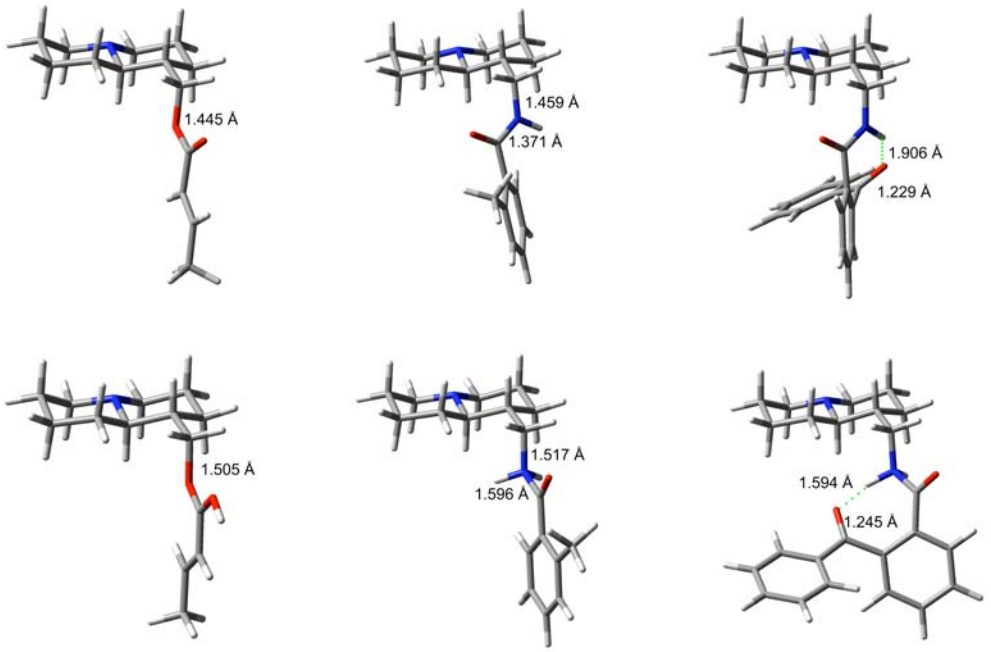

Figure 4. B3LYP/6-31G(d) optimized structures for neutral and protonated **3a**, **4a** and **4b**.

$[M+H]^+$ = 313,17330. Found $[M+H]^+$ = 313.17305. Diff. 2.5 × 10^{-4}. *Anal*. Calcd. for $C_{19}H_{24}N_2S$: C, 72.98; H, 7.68; N, 8.96. Found C, 72.73; H, 8.01; N, 8.60.

Acknowledgment. Some of the calculations presented in this document have been made with CSC's computing environment. CSC is the Finnish IT center for science and is owned by the Ministry of Education. Also Maija Lahtela-Kakkonen from University of Kuopio is thanked for helpful suggestions concerning the theoretical calculations.

REFERENCES

[1] Sadykov, A. S.; Aslanov, Kh. A.; Kushmuradov, Yu. K. *Alkaloidy khinolizidinovogo ryada. Khimiya*, stereokhimiya, biogenez Nauka, Moscow, 1975, pp 292 (in Russian).

[2] Wink, M. Methods in Plant Biochemistry, **1993**, *8*, 197.

[3] Tlegenov, R. T.; Dalimov, D. N.; Khaitbaev, Kh. Kh.; Abduvakhabov, A. A.; Uteniyazov, K. U. *Khimiya Prirod. Soedin*., **1990**, 513 (Chem.Nat.Compd.,1990 Engl.Transl.)

[4] Gafurova, Sh. M.; Abduvakhabov, A. A.; Aslanov, Kh. A. *Uzb. Khim. Zhurn*., **1979**, 56 (in Russian).

[5] Chang, M-Y.; Tai, H-M.; Lin, C-H.; Chang, N-C. *Heterocycles*, **2005**, *65*, 395.

[6] Tlegenov, R. T.; Aitmambetov, A. *Russ. J. Bioorg. Chem*., **2005**, *31*, 495.

[7] Galin, F. Z.; Kartsev, V. G.; Flekher, O. B.; Giniyatullina, G. V.; Tolstikov, G. A. *Chem. Nat. Compd*., **2004**, *40*, 569.

[8] Ma, S.; Ni B. *Chem. Eur.J*., **2004**, *10*, 3286.

[9] Collins, L.; Franzblau, S. G. *Antimicrob. Agents Chemother*, **1997**, *41*, 1004.

[10] Moini, M.; Jones, B. L.; Rogers, R. M.; Jiang, L. J. *J. Am. Soc. Mass Spectrom*. **1998**, *9*, 977.

[11] de Koning, L. J.; Nibbering, N. M. M.; van Orden, S. L.; Laukien, F. J.; *Int. J. Mass Spectrom. Ion Processes* **1997**, *165/166*, 209.

[12] Sheldrick, G. M. SHELXS-97, *Program for Crystal Structure Determination*, University of Göttingen, Göttingen, Germany, 1997.

[13] Sheldrick, G. M. SHELXS-97, *Program for Crystal Structure Refinement*, University of Göttingen, Göttingen, Germany, 1997**.**

[14] Gaussian 03, Revision C.02, Frisch, M. J.; Trucks, G. W.; Schlegel, H. B.; Scuseria, G. E.; Robb, M. A.; Cheeseman, J. R.; Montgomery, Jr., J. A.; Vreven, T.; Kudin, K. N.; Burant, J. C.; Millam, J. M.; Iyengar, S. S.; Tomasi, J.; Barone, V.; Mennucci, B.; Cossi, M.; Scalmani, G.; Rega, N.; Petersson, G. A.; Nakatsuji, H.; Hada, M.; Ehara, M.; Toyota, K.; Fukuda, R.; Hasegawa, J.; Ishida, M.; Nakajima, T.; Honda, Y.; Kitao, O.; Nakai, H.; Klene, M.; Li, X.; Knox, J. E.; Hratchian, H. P.; Cross, J. B.; Bakken, V.; Adamo, C.; Jaramillo, J.; Gomperts, R.; Stratmann, R. E.; Yazyev, O.; Austin, A. J.; Cammi, R.; Pomelli, C.; Ochterski, J. W.; Ayala, P. Y.; Morokuma, K.; Voth, G. A.; Salvador, P.; Dannenberg, J. J.; Zakrzewski, V. G.; Dapprich, S.; Daniels, A. D.; Strain, M. C.; Farkas, O.; Malick, D. K.; Rabuck, A. D.; Raghavachari, K.; Foresman, J. B.; Ortiz, J. V.; Cui, Q.; Baboul, A. G.; Clifford, S.; Cioslowski, J.; Stefanov, B. B.; Liu, G.; Liashenko, A.; Piskorz, P.; Komaromi, I.; Martin, R. L.; Fox, D. J.; Keith, T.; Al-Laham, M. A.; Peng, C. Y.; Nanayakkara, A.; Challacombe, M.; Gill, P. M. W.; Johnson, B.; Chen, W.; Wong, M. W.; Gonzalez, C.; and Pople, J. A.; Gaussian, Inc., Wallingford CT, 2004.

[15] GaussView 3.0, Gaussian, Inc., USA.